Fizika Nizkikh Temperatur, 2005, v. 31, No. 11, p. 1293–1301

Photoinduced absorption and anomalous dichroism in $NaCa_2Mn_2V_3O_{12}$ garnet as an evidence for the formation of oxygen holes dynamics

V.V. Eremenko, S.L. Gnatchenko, I.S. Kachur, V.G. Piryatinskaya, A.M. Ratner, and V.V. Shapiro

B. Verkin Institute for Low Temperature Physics and Engineering of the National Academy of Sciences of Ukraine, 47 Lenin Ave., Kharkov 61103, Ukraine
E-mail: piryatinskaya@ilt.kharkov.ua

M.B. Kosmyna, B.P. Nazarenko, and V.M. Puzikov

STC «Institute for Single Crystals» of the National Academy of Sciences of Ukraine 60 Lenin Ave., Kharkov 61001, Ukraine

Received April 27, 2005, revised May 25, 2005

It is shown that long-lived photoinduced dichroism in garnets is caused by photoproduced charges with anisotropic structure, keeping long memory of the pumping light polarization, while photoinduced absorption is due to all photoproduced charges irrespective of their intrinsic structure. The charges with anisotropic structure are identified as two-center oxygen holes. The formation of an oxygen hole is preceded by the excitation of a charge-transfer state with electron partially transferred to a cation C (V^{5+} for $NaCa_2Mn_2V_3O_{12}$ garnet) from an adjacent oxygen anion. To turn this excited state into a free hole state requires some time τ_{hole} during which the hole axis can be reoriented resulting in a diminution of dichroism. The time τ_{hole} shortens with increasing ionization potential of the cation C (very high for V^{5+}). Such a mechanism explains qualitatively a set of unusual experimental facts, in particular, a very strong dichroism observed just in the $NaCa_2Mn_2V_3O_{12}$ garnet, where photoinduced changes of all optical properties disappear after switching off of the irradiation significantly faster than those in other garnets examined.

PASC: **78.40.-q**

1. Introduction

Long-lived photoinduced phenomena in magnetic insulators have been extensively studied (e.g., [1–10]) and associated with the photoinduced transfer of charges. In ferromagnets or ferrimagnets, whose Curie temperature exceeds the upper temperature limit of the existence of long-lived photoinduced phenomena, photoinduced changes in optical properties can be observed only simultaneously with changes in magnetic structure (in particular, illumination of the yttrium iron garnet $Y_3Fe_5O_{12}$ with linearly polarized light affects the magnetic anisotropy [1–3], domain structure [4], and optical dichroism [3]). The photoinduced changes in optical and magnetic properties are deeply interconnected, which strongly complicates their mechanism and hampers its elucidation.

To separate photoinduced changes of optical properties from those of magnetic characteristics, the authors [5–10] recently examined antiferromagnetic garnets ($Ca_3Mn_2Ge_3O_{12}$, $NaCa_2Mn_2V_3O_{12}$ with a low Néel temperature $T_N \sim 20$ K) and the paramagnetic garnet $Ca_3Ga_{2-x}Mn_xGe_3O_{12}$ in a broad temperature region below the temperature of disappearance of long-lived photoinduced phenomena (of about 150 K). In the absence of magnetic ordering, photoinduced optical phenomena in the set of garnets mentioned have common well-pronounced features, which enabled us to elucidate their nature [5–8].

For all the garnets examined, $Ca_3Mn_2Ge_3O_{12}$, $NaCa_2Mn_2V_3O_{12}$ and $Ca_3Ga_{2-x}Mn_xGe_3O_{12}$ ($x = 0.01$ and 0.02), a photoinduced addition to absorption, ΔK, and photoinduced dichroism were observed and ana-

lyzed. It was found that the corresponding relaxation curves, recorded after switching off the irradiation, are of similar character. Each relaxation curve contains a continuous set of exponential decay components with decay time varying in a range from a minute up to many hours (a special analysis proved that decay times fill in this interval continuously [7]). As temperature rises, the observed decay kinetics does not change noticeably, while ΔK diminishes by an order of magnitude. Such decay kinetics cannot be ascribed to some new irradiation-produced optical centers but is naturally explained by random electric fields of photoproduced localized charges. These fields play a dual role: they enhance the optical transition observed and strongly promote delocalization of holes, thus accelerating their recombination with negative charges (localized electrons). A broad continuous set of decay times is conditioned by a continuous distribution of random electric fields over magnitude. Such notion was quantitatively corroborated by the solution of the corresponding kinetic equation with realistic values of parameters [5,6].

Photoinduced dichroism, observed simultaneously with photoinduced absorption ΔK, has the same relaxation kinetics but, unlike ΔK, sharply grows when changing from $Ca_3Mn_2Ge_3O_{12}$ or $Ca_3Ga_{2-x}Mn_xGe_3O_{12}$ to $NaCa_2Mn_2V_3O_{12}$ (when varying the polarization direction of the pump light, the difference $\Delta K_{\max} - \Delta K_{\min}$ between the maximum and minimum values of ΔK amounts to 90 % of $\Delta K_{\max}$ for $NaCa_2Mn_2V_3O_{12}$ and 10 to 20 % only for other mentioned garnets). These and other facts inspired a mechanism of long-lived photoinduced dichroism caused by two-center oxygen holes whose axis direction keeps long memory of the pump polarization direction [7,8]. This mechanism is stated in Sec. 2.

The purpose of the present paper is to corroborate the proposed mechanism by new experimental data described in Sec. 3. The main experimental result consists in separating the optical manifestations of photoproduced charges of opposite signs: electrons localized on lattice cations cause photoinduced absorption only, while two-center oxygen holes are responsible both for photoinduced dichroism and absorption. The comparison of dichroism and absorption, caused by opposite-sign charges, makes it possible to specify and confirm the proposed mechanism of dichroism recorded through two-center holes when pumping a crystal with polarized light. Such analysis is carried out in Sec. 4.

2. Main notion to be corroborated by experiment

Prior to the description of experiment, in order to elucidate its goals, it seems helpful to summarize the main relevant notion that is based on our previous results [7,8] and has to be corroborated by new experiments stated in Sec. 3. This notion consists in the following.

(i) The role of oxygen holes as photoproduced charges in the formation of photoinduced absorption and dichroism follows from different independent considerations [7,8]. First, the motion and subsequent recombination of photoproduced charges is mirrored by the relaxation kinetics of photoinduced changes after switching off of the irradiation. A similarity of relaxation curves, observed for garnets $Ca_3Mn_2Ge_3O_{12}$, $Ca_3Ga_{2-x}Mn_xGe_3O_{12}$, $NaCa_2Mn_2V_3O_{12}$ with different cation composition and the same anion group O_{12} , suggests a predominant role of the O^{2-} anion subsystem in the motion of photoproduced charges. This means that irradiation creates holes (O^-) moving in the oxygen subsystem.

Second, there is no alternative for the nature of photoproduced positive charges. Indeed, in all the garnets examined photoinduced absorption can be excited by red light with photon energy (of about 2 ev) much less than the ionization potential of every lattice cation (> 30 eV) but comparable with the dielectric gap, E_g, of the O^{2-} sublattice (an estimate $E_g \approx 2$ eV follows from the absorption spectrum given below in Fig. 1).

(ii) The structural features of holes in the oxygen subsystem of garnets are predetermined by a closed-shell configuration of O^{2-} ion identical with that of Ne. It was well established that in solid neon, as well as in other rare-gas solids, the stable lowest state of the hole ns^2np^5 is a two-atom molecule ns^2np^5–ns^2np^6 formed on adjacent lattice sites. The atomic valence p-hole, distributed between two atoms, realizes a strong exchange binding of the scale of 1 eV [11,12]. The magnitude of such exchange binding mainly depends on the ratio of the valence p-state radius to the interatomic distance in the ideal lattice. This ratio amounts to about 0.3 for the garnets considered, to 0.17 for solid neon, and to 0.25 for solid argon. For alkali halides (KCl, KI, NaI), where the existence of stable two-center holes in the anion subsystem is also reliably established, this ratio varies from 0.20 to 0.27. Hence, stable two-atom hole polarons must exist also in the O^{2-}-subsystem of garnets.

(iii) Only charges with anisotropic structure can retain a long memory of the pumping polarization direction and, hence, be responsible for long-lived photoinduced dichroism observed. A two-center hole in the oxygen subsystem is the only realistic version of charge with anisotropic structure in garnets.

It is easy to trace how two-center holes, created by polarized illumination, cause dichroism. The latter is described by the difference, $\Delta K_\perp - \Delta K_\parallel$, in photo-

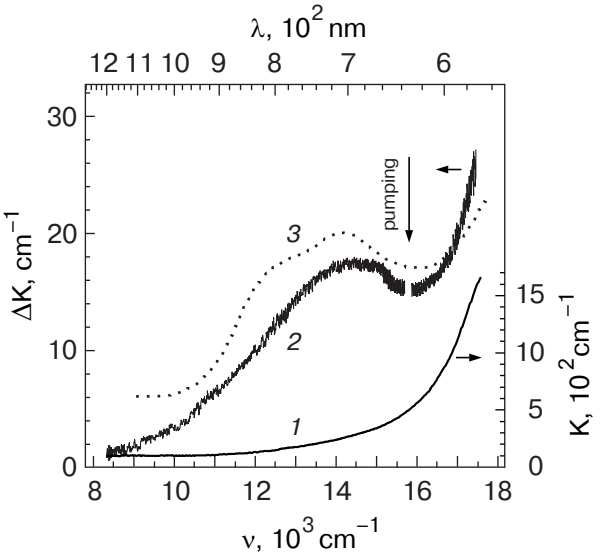

Fig. 1. Absorption spectrum of garnet $NaCa_2Mn_2V_3O_{12}$ with five-valence vanadium at 30 K: without pumping (curve *1*) and the photoinduced addition to absorption under pumping (curve *2*); the pumping light frequency is shown by an arrow, and the small spectral gap near it is caused by a light filter suppressing the scattered pump light) [9]. For comparison, dotted line *3* shows the absorption spectrum of garnet $NaCa_2Mg_2V_3O_{12}$ with four-valence vanadium [13]. The comparison of the curves *2* and *3* indicates that the photoinduced absorption of $NaCa_2Mn_2V_3O_{12}$ at $\nu < 16000$ cm^{-1} is due to V^{5+}-ions turned to V^{4+} via the taking away of an electron from O^{2-}.

induced absorption measured with the probe light polarized perpendicular to and parallel to the pump light polarization. The photoinduced addition to absorption, ΔK, is determined by the photoinduced field **F** enhancing a weak optical transition in the lattice ions (obviously, Mn^{3+} or Mn^{4+}) serving as probe optical centers. The field **F** is produced mainly by a two-center hole, lying in the first coordination sphere of the probe ion A, and is perpendicular to the two-center hole axis (Fig. 2). Since the axis is oriented predominantly parallel to the pump polarization direction, probe light experiences a stronger additional absorption if polarized perpendicularly to the pump polarization. Hence, $\Delta K_\perp > \Delta K_\parallel$ in accordance with experiment (see Sec. 3).

(iv) The magnitude of dichroism is obviously dictated by the reorientation of the axes of two-center holes created by polarized light. Experiment shows that the reorientation of the axes of two-center holes after the completion of their creation is not of great importance. Indeed, a very strong dichroism, much greater than that in other garnets examined, is observed in $NaCa_2Mn_2V_3O_{12}$ garnet, where dichroism disappears after switching off of the irradiation significantly faster than in other garnets. Thus, of the most importance is the reorientation of the axes of two-center holes in the course of their creation by polarized light that occurs in the following way.

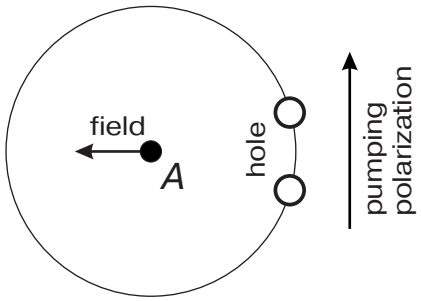

Fig. 2. Origin of photoinduced dichroism: a two-center oxygen hole, allocated in the first coordination sphere of the probe manganese ion A, creates at the point A electric field perpendicular to the two-center hole axis and to the polarization direction of the pump.

The initial excitation, caused by pump light polarized in the *z* direction, rearranges the binding between a lattice cation C (identified below as vanadium for $NaCa_2Mn_2V_3O_{12}$) and an adjacent anion O^{2-} lying on the *z* axis with respect to ion C. Such excitation is of charge-transfer character: an electron is partially transferred from O^{2-} to cation C having a high ionization potential. Such excited state, denoted as $<j = 1|$, is one of 6 degenerate states related to 6 oxygen ions in the first coordination sphere of ion C. Every excited state $<j|$ can pass during a time τ_{hole} to another type of excitation, energetically positioned somewhat lower, with the completed electron transfer: a free hole appears in the oxygen sublattice and the cation C involved has some charge less by unity than that in regular sites. Along with this, every excited state $<j|$ can pass during a time τ_j to another of 6 degenerate states $<j'|$ (such transitions are caused by random photoinduced electric fields absent in the ideal lattice Hamiltonian with orthogonal eigenstates $<j|$). Under pumping with polarized light, the strongest possible dichroism takes place if $\tau_{hole} << \tau_j$. In the opposite case $\tau_{hole} >> \tau_j$, all the states $<j|$ become equally populated (as under unpolarized pumping), so that dichroism vanishes. Thus, the cause of the anomalous dichroism observed in $NaCa_2Mn_2V_3O_{12}$ sought be searched in a small magnitude of the time τ_{hole} required for charge-transfer excitation to be transformed into an oxygen hole (the time τ_j, dictated by random fields, is nearly the same for all garnets). In Sec. 4 it will be elucidated why τ_{hole} takes on the lowest value in just the $NaCa_2Mn_2V_3O_{12}$ garnet.

3. Experiment

3.1. Experimental technique

Single crystals of $NaCa_2Mn_2V_3O_{12}$ garnet were grown from melt solution by the method of spontaneous crystallization [10]. A sample was cut in the form of a (50±10) μm thick plane-parallel plate perpendicular to the [100] direction. Photoinduced phenomena were examined with an optical double-beam setup. The sample was illuminated by a He–Ne laser (with light wavelength of $\lambda = 633$ nm and flux density of 0.13 W/cm^2). A stable wide-band emission of an arc xenon lamp, dispersed through a monochromator, served as a probe light. The intensity of the probe beam was low enough to cause no photoinduced phenomena. A special light filter was applied to suppress scattered illumination from the laser. The intensity of probe light passed through the sample was detected by a photoelectron multiplier. The photoinduced absorption coefficient is defined as $\Delta K = (1/d)\ \ln(I_0/I)$, where d is the plate thickness, and I_0 and I denote the intensity of the probe beam passed through the plate being in the ground state or exposed to irradiation, respectively (photoinduced changes in reflection coefficient are not observed).

The absorption spectrum of the illuminated sample was registered under pumping lasting 15 min (such time interval is sufficient for the photoinduced effect to reach saturation).

To examine photoinduced dichroism, probe light was polarized in the lattice direction [110] and the photoinduced addition to absorption coefficient was measured under irradiation with light polarized parallel ($\Delta K_\parallel$) and perpendicular ($\Delta K_\perp$) to the probe light polarization. Photoinduced dichroism is defined as the difference $\Delta K_\perp - \Delta K_\parallel$.

3.2. Spectra of photoinduced absorption and dichroism

The absorption spectrum of the garnet $NaCa_2Mn_2V_3O_{12}$, measured in the absence of pumping, is shown in Fig. 1 (curve *1*). The figure presents a long-wavelength tail of a strong absorption that is fast growing with increasing frequency (the position of the absorption band maximum, lying in the region of a very strong absorption, could not be determined). To all appearance, this absorption band is formed with the participation of manganese ions. Indeed, the garnet $NaCa_2Mg_2V_3O_{12}$, differing from the $NaCa_2Mn_2V_3O_{12}$ garnet considered by the replacement of Mn by Mg only, is transparent in the same spectral region [13]. On the other hand, such a broad absorption band cannot be assigned to d–d transitions inside Mn subsystem, which manifest themselves as narrow absorption bands. The broad absorption band observed can be attributed to charge transfer transitions between Mn ion and its crystalline surroundings (probably, adjacent oxygen anions). Note that photoinduced dichroism considered below is connected with this absorption band.

Figure 1 also presents the spectrum of additional absorption caused by illumination (curve *2*) [9]. For comparison, the dotted curve shows the absorption spectrum of the garnet $NaCa_2Mg_2V_3O_{12}$ exposed to thermal quenching that lowers the valence of a part of V^{5+} cations from 5 down to 4 [13] (in regular crystals $NaCa_2Mn_2V_3O_{12}$ and $NaCa_2Mg_2V_3O_{12}$, vanadium is present in the form of V^{5+}). According to [13], transitions in V^{4+} ions manifest themselves in the absorption band shown by the dotted curve in Fig. 1. A close similarity of the photoinduced absorption band, observed in $NaCa_2Mn_2V_3O_{12}$ near $\nu = 14300$ cm^{-1}, with the absorption band of V^{4+} ions in $NaCa_2Mg_2V_3O_{12}$, leads to a conclusion that in the former case this photoinduced absorption band belongs to photoproduced V^{4+} ions [9]. Thus, the photoproduction of an oxygen hole is realized through the localization of an electron, taken away from an O^{2-} anion, on a V^{5+} cation.

Figure 3 presents the spectrum of photoinduced dichroism described by the difference, $\Delta K_\perp - \Delta K_\parallel$, between absorption measured with probe light polarized perpendicular to and parallel to the pump light polarization. As can be seen from the figure, this dichroism has a maximum at the point ν=16700 cm^{-1} lying within the absorption band of manganese. Near this maximum, $\Delta K_\perp$ exceeds $\Delta K_\parallel$ by an order of magnitude. This provides direct evidence that photoinduced absorption of probe light by manganese ions is highly sensitive to the angle between the polarizations of the probe and pump lights (Sec. 2, Item iii, Fig. 2).

On the contrary, the absorption band of V^{4+} ions (shown in Fig. 1) is not sensitive to the polarizations of the pump and probe rays. Indeed, although the absorption of V^{4+} ions makes noticeable contributions to the curves $\Delta K_\perp$ and $\Delta K_\parallel$ presented in Fig. 3,*a*, these contributions are equal and disappear from the difference curve shown in Fig. 3,*b*. Really, this difference curve has no maximum at the point $\nu = 14000$ cm^{-1} related to the absorption of V^{4+} ions and distinctly seen in Fig. 1 (curves *2* and *3*). A noticeable dichroism, observed at $\nu \le 14000$ cm^{-1}, bears no relation to the absorption of V^{4+} ions and is due to the long-wavelength tail of the manganese absorption sensitive to the pump polarization. We will return to this fact in Sec. 4.

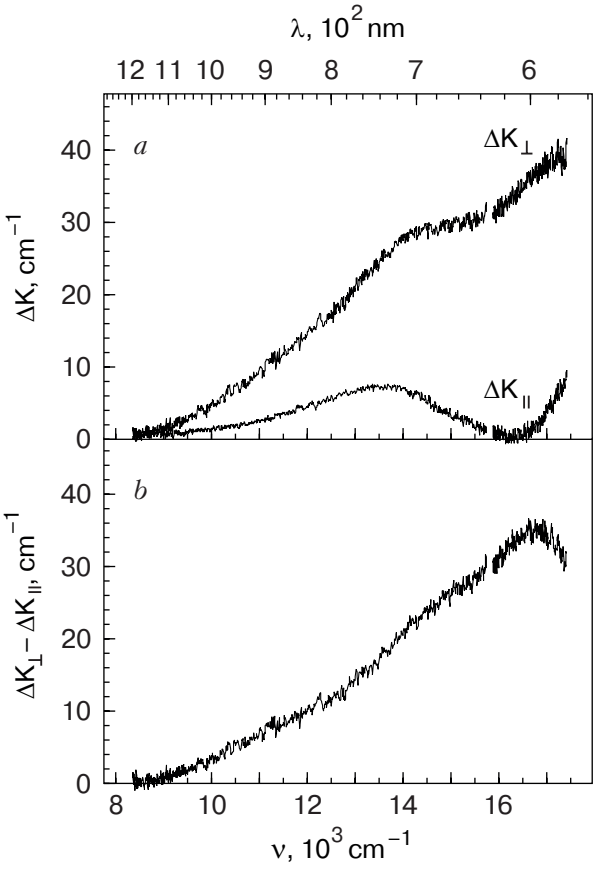

Fig. 3. The spectrum of photoinduced addition to absorption $NaCa_2Mn_2V_3O_{12}$ under irradiation with light polarized perpendicular and parallel to the probe light polarization ($\Delta K_\perp$ and $\Delta K_\parallel$, respectively) at 30 K (*a*). The difference spectrum, $\Delta K_\perp - \Delta K_\parallel$, describing the dichroism of $NaCa_2Mn_2V_3O_{12}$ (*b*).

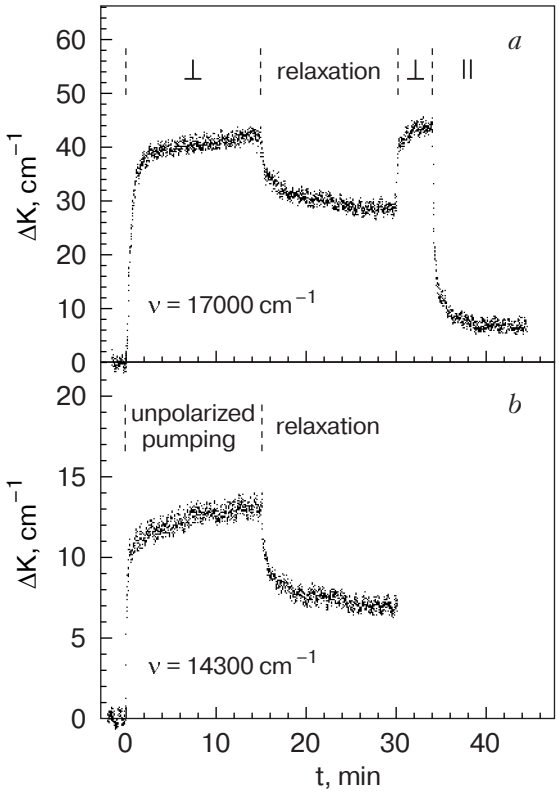

Fig. 4. Time dependence of the photoinduced addition to absorption coefficient, ΔK, at T = 40 K measured at different frequencies: 17000 cm^{-1} (*a*) and 14300 cm^{-1} (*b*) under pumping conditions changed as indicated in the figure. The symbol ⊥ or ∥ denotes a time interval when the sample was irradiated with light polarized perpendicular to or parallel to the probe light polarization. The relaxation regime in the absence of pumping is also shown.

3.3. Kinetics of photoinduced dichroism and absorption

Figure 4,*a* demonstrates the measured dichroism and its kinetics under changing conditions of pumping. At first, the photoinduced addition to absorption, $\Delta K_\perp$, was measured under pumping polarized perpendicularly to the probe light polarization. Then, at t = 15 min when photoinduced dichroism nears its saturation value, the pump was switched off and the relaxation of $\Delta K_\perp$ was observed during the next 15 min. At t = 30 min the perpendicularly polarized pump was switched on again for 5 min, which was sufficient to achieve the same level of $\Delta K_\perp$ as before the pump had been switched off. At t = 35 min the pump polarization direction was switched parallel to the probe light polarization, causing the diminution of ΔK down to a small value $\Delta K_\parallel \approx 0.1 \Delta K_\perp$; this indicates on a high degree of dichroism $\Delta K_\perp / \Delta K_\parallel \approx 10$.

For comparison, Fig. 4,*b* shows the time dependence of the photoinduced absorption observed under unpolarized pumping at the frequency ν = 14300 cm^{-1}, i.e., at the maximum of the photoinduced absorption band of V^{4+} centers insensitive to the polarization of the pump (see Sec. 2). As seen from the comparison of Figs. 4,*b* and 4,*a*, the polarization of the pump influences only the magnitude of photoinduced absorption but not its kinetics under irradiation or after the irradiation is switched off. In more detail, such comparison will be carried out in Sec. 4.

It is also helpful to compare the relaxation rate of photoinduced absorption, observed at a low temperature after switching off of the irradiation in two garnets: in the garnet $NaCa_2Mn_2V_3O_{12}$ with a strong dichroism, and in the garnet $Ca_3Mn_2Ge_3O_{12}$ with a weak dichroism [5]. To that end, making allowance for the close similarity between the relaxation kinetics of photoinduced absorption and dichroism, let us define the mean relaxation rate as

$$R_{\text{relax}} = [\Delta K(0) - \Delta K(20 \text{ min})] / \Delta K(0) \qquad (1)$$

where time is counted from the switching off of the irradiation. Fig. 4 gives $R_{relax} \approx 0.35$ for $\Delta K_\perp$ in $NaCa_2Mn_2V_3O_{12}$. The value of R_{relax} in $Ca_3Mn_2Ge_3O_{12}$, equal to about 0.12 [5,6], indicates on a considerably slower relaxation.

3.4. Temperature dependence of photoinduced dichroism and absorption

Figure 5 shows the temperature dependence of dichroism $K_{dich} \equiv \Delta K_\perp - \Delta K_\parallel$ ($\Delta K_\perp$ and $\Delta K_\parallel$ were measured under irradiation lasting long enough that $\Delta K_\perp$ and $\Delta K_\parallel$ become independent of time). For comparison, the temperature dependence of the same quantity for $Ca_3Mn_2Ge_3O_{12}$ [5] is plotted by the dashed the line. Figure 5 demonstrates different temperature behavior of dichroism for $NaCa_2Mn_2V_3O_{12}$ and $Ca_3Mn_2Ge_3O_{12}$. For $NaCa_2Mn_2V_3O_{12}$, K_{dich} decreases with temperature within the total temperature interval examined, quite similarly to photoinduced absorption ΔK observed under unpolarized pumping. For $Ca_3Mn_2Ge_3O_{12}$, K_{dich} diminishes with increasing temperature above the point $T_{dim} = 90$ K only, while the temperature behavior of ΔK is quite similar for both garnets. For these garnets, Table 1 presents T_{dim} together with the degree of dichroism $\Delta K_\perp / \Delta K_\parallel$ and relaxation rate (1).

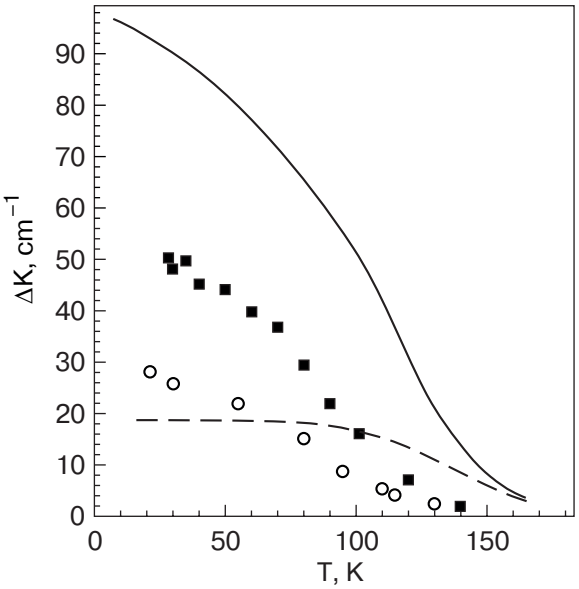

Fig. 5. Temperature dependence of photoinduced dichroism $\Delta K_\perp - \Delta K_\parallel$ measured for $NaCa_2Mn_2V_3O_{12}$ under polarized pumping (squares). The temperature dependence of photoinduced absorption measured under unpolarized pumping (circles) is of the same character. For comparison, the corresponding dependences of photoinduced dichroism and photoinduced absorption for garnet $Ca_3Mn_2Ge_3O_{12}$ [5] are shown by dashed and solid lines, respectively.

Table 1. Characteristics of dichroism for the two garnets: relative degree of dichroism, the commencement T_{dim} of its temperature diminution, and the relaxation rate (1).

Garnet	$\Delta K_\perp / \Delta K_\parallel - 1$	T_{dim}, K	R_{relax}
$NaCa_2Mn_2V_3O_{12}$	9	*	0.35
$Ca_3Mn_2Ge_3O_{12}$	0.2	90	0.12

C o m m e n t: *Dichroism decreases with temperature in all of the region examined

4. Corroboration of the mechanism of photoinduced dichroism and of the role of two-center holes

4.1. General conception of the enhancement of optical transitions by electric fields of photoproduced charges

As was mentioned in Introduction, long-lived photoinduced phenomena in garnets are generally caused by the enhancement of optical transitions in the manganese subsystem by the electric field of photoproduced charges [5,6]. In $NaCa_2Mn_2V_3O_{12}$ garnet, along with such photoinduced contribution to absorption at $\nu \geq 16000$ cm^{-1} (Fig. 3), irradiation creates V^{4+} centers which give rise to the photoinduced absorption band near 14000 cm^{-1} (Fig. 1). The proposed mechanism of photoinduced absorption is illustratively corroborated by a comparison of these photoinduced contributions to absorption in $NaCa_2Mn_2V_3O_{12}$ garnet.

Under irradiation with polarized light, an anisotropic electric field of two-center holes, influencing optical transitions in the manganese subsystem, causes a sharp dichroism of photoinduced absorption at $\nu \approx 17000$ cm^{-1} (Fig. 3). Note that these transitions can occur in all manganese ions being, enhanced by the applied field by a value proportional to the number of charges. But the V^{4+}-absorption, proportional to a small photoproduced portion of V^{4+} ions, is practically insensitive to the field of photoproduced charges: this field changes the V^{4+}-absorption by a negligibly small value quadric in the number of charges. Being insensitive to the anisotropic field of photoproduced two-center holes, the V^{4+}-absorption exhibits no dichroism, is was spectroscopically evidenced in Sec. 3.2.

Thus, two different ions, labeled as C and A, are involved in photoinduced phenomena. Ion C (V^{5+} for $NaCa_2Mn_2V_3O_{12}$ garnet) participates in the creation of oxygen hole O^- via the taking away of an electron from an adjacent O^{2-} cation. The created hole O^- undergoes two-site self-trapping and turns to a two-center hole with the initial orientation of the axis. Then

the two-center hole, retaining its axis direction, gets to the first coordination sphere of the probe ion A (≡ Mn) sensitive to the electric field of the hole and, hence, to its axis direction, which conditions dichroism. Note that V^{5+} ions with a very high ionization potential cannot play the role of probe ion A, since the oxygen holes created are more strongly attracted by Mn ions, with a much lower ionization potential.

4.2. Creation of oxygen holes through complete transfer of electron from O^{2-} anion to V^{5+} cation

As was shown in Sec. 3.2, an oxygen hole is created through the taking away of an electron from a O^{2-} anion and localizing it on a V^{5+} cation. Hence it follows that the number of photoproduced oxygen holes coincides with that of V^{4+} ions. This coincidence can be proved by the comparison of the absorption band of V^{4+} ions, created by unpolarized pumping with maximum at $\nu \approx 14000$ cm^{-1} (Fig. 1), with the absorption band of two-center oxygen holes created by pumping with light polarized perpendicularly to the polarization of the probe light (the reorientation of two-center holes after their creation can be neglected; see Sec. 4.3). The ratio of the maximum ordinates of these absorption bands, $\rho = \Delta K_\perp(17000)/\Delta K$ (14300), must be independent of the number of holes and, hence, of temperature and irradiation time. Figure 6 presents the ratio $\rho = \Delta K_\perp(17000)/\Delta K$ (14300) observed under pumping and in the course of the subsequent relaxation. This ratio, measured under pumping with the same intensity, was found, within the accuracy of measurements, to be independent of temperature in the region examined, 40K ≤ T ≤ 80 K. After switching off of the irradiation, ρ increases slightly, which provides an additional evidence for the reorientation of holes on the stage of their creation (see Sec. 4.4, Item ii).

The constancy of the ratio ρ confirms that oxygen holes are created through the trapping of an electron, taken away from an O^{2-}-ion, by an adjacent vanadium cation of the lattice.

4.3. Conservation of the orientation of two-center holes after their formation

Experiment does not detect the reorientation of the axes of two-center holes after the completion of their formation. Indeed, as seen from Fig. 6, after switching off of the irradiation, the dichroism relaxes (disappears) with the same rate (or even slightly slower) than the number of photoproduced charges. If this relaxation were accompanied by the reorientation of the axes of two-center holes, the dichroism would diminish faster than the number of photoproduced charges, and the ratio $\rho = \Delta K_\perp$ (17000)/ΔK (14300), presented in Fig. 6, would be a decreasing function of time after the switching off of the irradiation.

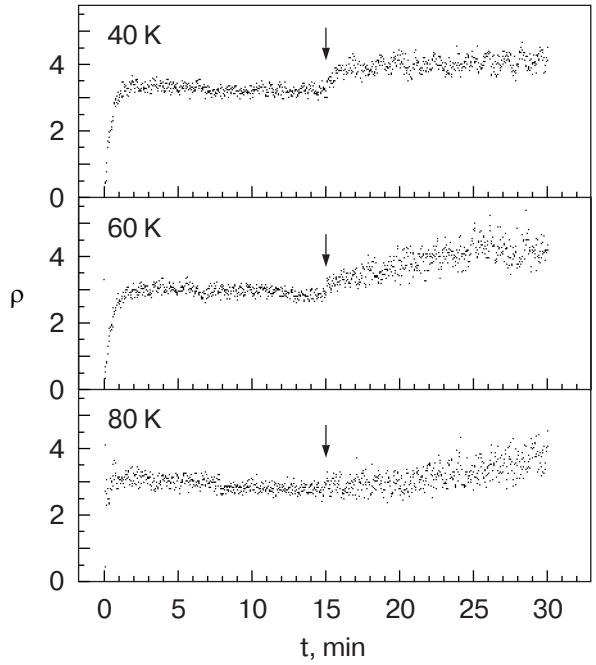

Fig. 6. Ratio $\rho = \Delta K_\perp$ (17000 cm^{-1})/ΔK(14300 cm^{-1}) measured under pumping and in the course of the subsequent relaxation at different temperatures (the moment of switching off of the irradiation is indicated by an arrow). This ratio mainly reproduces the ratio of the number of photoproduced oxygen holes to that of photoproduced V^{4+}-ions. The approximate constancy of ρ confirms that oxygen holes are created through the trapping of an electron, taken away from an O^{2-}-ion, by an adjacent V^{5+}-cation (a slight enhancement of ρ after the switching off of the irradiation is explained in Sec. 4.4, Item (ii)).

Thus, Fig. 6 demonstrates that the time, τ_{reor}, required for a two-center hole to be reoriented, greates exceeds the time of the hole–electron recombination dictated by the hole hopping time τ_{hop}:

$$\tau_{reor} >> \tau_{hop}. \qquad (2)$$

Note that for two-center holes observed in alkali halide crystals the inequality (2) was experimentally established as well [14–16].

The physical reason for the relation (2) is elucidated by Fig. 7. Initially, a two-center hole was located on atoms A and B indicated by bold circles; the orbital of the *p*-hole at every atom (the absent *p*-electron) is schematically shown by thin line. Immediately after a hop, the two-center hole occupies a new position BC or BD with the same orientation of the axes of the atomic *p*-holes. (In the latter case, the subsequent reorientation of the hole axis in the direction BD does not affect the hopping probability). The hop creating hole BD is much less probable than the hop

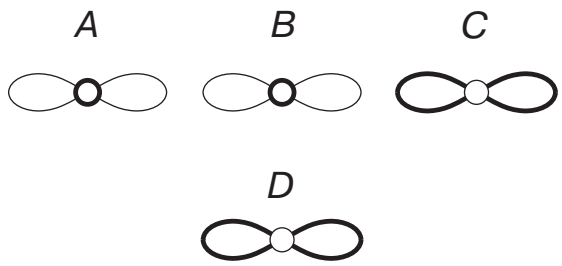

Fig. 7. Motion of a two-center hole, initially allocated on the atoms A and B, to a next position BC or BD. The motion rate is determined by the overlap of the atomic *p*-orbital not occupied at the atom B (thin line) with its orbital occupied at adjacent atoms (bold line); hence, the hop AB–BD has much lower probability. In the latter case the hop is followed (in order to lower the resonance energy) by a reorientation the axes of the atomic *p*-holes and, hence, of the axis of the two-center hole.

creating hole BC. Indeed, the probability of hopping sharply depends on the exchange interaction between atom B and the adjacent atom C or D [17], the exchange BC being much stronger due to a greater overlap of wave-functions.

4.4. Reorientation of the axes of oxygen holes in the course of their creation by polarized light

Experimental data corroborate the reorientation mechanism, stated in Sec. 2 (Item 4). This mechanism involves excited states $<j|$ (j = 1,..., 6) formed by a partial electron transfer to cation C from any of 6 adjacent O^{2-} ions. The efficiency of this mechanism is characterized by the time ratio

$$u = \tau_{\text{hole}} / \tau_j \qquad (3)$$

where τ_j is the time of the transition between degenerate states $<j|$; the time τ_{hole} is required for a complete electron transfer to ion C, resulting in the formation of a free oxygen hole. (As was shown in Sec. 4.2, for $NaCa_2Mn_2V_3O_{12}$ the ion C should be identified with V^{5+}). Let us trace how the variation of the numerator and denominator in (3) affects the dichroism.

(i) The reorientation of two-center holes is due to transitions between its excited states caused by random electric fields of photoproduced charges (in the ideal lattice, the degenerate states $<j|$ are orthogonal to one another). These fields have a large straggling in magnitude, which is mirrored by the relaxation kinetics after switching off of the irradiation (Fig. 4): two-center holes, formed at the places of a strong field, disappear rapidly and form the initial steep part of the relaxation curve, while its gently sloping part corresponds to holes formed at the places of a weak field. In the latter case, the reorientation rate, commensurable with the magnitude of random fields, is significantly lower. Thus, the gently sloping part of the relaxation curve pertains to holes that have undergone a weak reorientation in their creation stage. This is mirrored by a slight enhancement of the ratio $\rho = \Delta K_{\perp}$ (17000)$/\Delta K$ (14300) with an increase of time counted from the moment of switching off of the irradiation (Fig. 6).

(ii) Figure 5 presents the temperature dependences of photoinduced absorption and dichroism for $NaCa_2Mn_2V_3O_{12}$ (marks) and $Ca_3Mn_2Ge_3O_{12}$ (lines). As seen from the figure, photoinduced absorption and dichroism vary with temperature in a similar way for $NaCa_2Mn_2V_3O_{12}$ and in a different manner for $Ca_3Mn_2Ge_3O_{12}$. Such a distinction between two garnets can be explained in terms of the ratio (3). An increase of temperature promotes overcoming the energy barrier between the initial excited state $<j|$ and the state with a free hole, so that the hole creation time τ_{hole} must shorten with increasing temperature. On the contrary, the time, τ_j , of the transitions between the degenerate excited states is determined by random fields which cannot noticeably depend on temperature. Hence, an increase of temperature entails a decrease of the ratio (3) and a diminution of the reorientation of two-center holes in the stage of their creation, which compensates the temperature acceleration of the recombination of photoproduced charges after their creation. In the case of garnet $Ca_3Mn_2Ge_3O_{12}$, where the reorientation mechanism acts very efficiently (see Table 1), this effect is well pronounced and results in a weakened temperature dependence of dichroism within a rather broad temperature interval $T < T_{\text{dim}}$ = 90 K (Fig. 5). But for $NaCa_2Mn_2V_3O_{12}$, the reorientation mechanism manifests itself very weakly and cannot cause a noticeable difference between the temperature dependences of dichroism and photoinduced absorption. Thus, the comparison of photoinduced phenomena in $NaCa_2Mn_2V_3O_{12}$ and $Ca_3Mn_2Ge_3O_{12}$ (a different temperature behavior of dichroism explainable only in terms of the initial stage of the oxygen hole formation) corroborates the mechanism of the creation and reorientation of two-center holes stated in Sec. 2, Item iv.

(iii) A sharp difference in dichroism, observed in $NaCa_2Mn_2V_3O_{12}$ and $Ca_3Mn_2Ge_3O_{12}$ (see Table 1), can be also understood in terms of relation (3) involving excited states $<j|$ with a partial electron transfer to the ion C from adjacent O^{2-} ions. The degree of this electron transfer is dictated by the attractive potential of the ion C, which is commensurate with the ionization potential I_C of the separate ion C. On the other hand, the greater is the portion of an electron transferred to the cation C from an adjacent O^{2-} anion in an excited state, the easier the electron can be comp-

Table 2. Ionization potentials of free ions of garnet constituents

Garnet	$Ca_3Mn_2Ge_3O_{12}$			$NaCa_2Mn_2V_3O_{12}$			
Cation	Ca^{2+}	Mn^{3+}	Ge^{4+}	Na^+	Ca^{2+}	Mn^{2+}	$C=V^{5+}$
Ionization potential (eV)	I_2=11.9	I_3=33.7	I_4=45.7	I_1=5.1	I_2=11.9	I_2=15.6	I_5=65.3

letely localized at the ion C, resulting in the generation of a free oxygen hole. Thus, with an increase of I_C the hole formation time τ_{hole} shortens, which leads to a diminution of the oxygen hole reorientation and to the corresponding enhancement of dichroism. For garnets $Ca_3Mn_2Ge_3O_{12}$ and $NaCa_2Mn_2V_3O_{12}$, Table 2 presents the *n*th ionization potential of each *n*-valence cation taken in a free state. The cation V^{5+}, playing the role of the ion C in $NaCa_2Mn_2V_3O_{12}$, has ionization potential of 65 eV, significantly exceeding the ionization potential of every cation of $Ca_3Mn_2Ge_3O_{12}$. The corresponding difference in the hole formation time τ_{hole} explains the strong difference in dichroism observed in $NaCa_2Mn_2V_3O_{12}$ and $Ca_3Mn_2Ge_3O_{12}$.

1. R.W. Teale and D.W. Temple, *Phys. Rev. Lett.* **19**, 904 (1967).
2. R.F. Pearson, A.D. Annis, and P. Kompfner, *Phys. Rev. Lett.* **21**, 1805 (1968).
3. J.F. Dillon, E.M. Gyorgy, and J.P. Remeika, *Phys. Rev. Lett.* **23**, 643 (1969).
4. V.F. Kovalenko, E.S. Kolezhuk, and P.S. Kuts, *JETP* **54**, 742 (1981).
5. V.V. Eremenko, S.L. Gnatchenko, I.S. Kachur, V.G. Piryatinskaya, A.M. Ratner, and V.V. Shapiro, *Phys. Rev.* **B61**, 10670 (2000).
6. V.V. Eremenko, S.L. Gnatchenko, I.S. Kachur, V.G. Piryatinskaya, A.M. Ratner, V.V. Shapiro, M. Fally, and R.A. Rupp, *Low Temp. Phys.* **27**, 22 (2001).
7. V.V. Eremenko, S.L. Gnatchenko, I.S. Kachur, V.G. Piryatinskaya, A.M. Ratner, M.B. Kosmyna, B.P. Nazarenko, and V.M. Puzikov, *J. Phys.: Condens. Matter* **15**, 4025 (2003).
8. V.V. Eremenko, S.L. Gnatchenko, I.S. Kachur, V.G. Piryatinskaya, A.M. Ratner, M.B. Kosmyna, B.P. Nazarenko, and V.M. Puzikov, *Phys. Rev.* **B69**, 233102 (2004).
9. S.L. Gnatchenko, V.V. Eremenko, I.S. Kachur, V.G. Piryatinskaya, V.V. Slavin, V.V. Shapiro, M.B. Kosmyna, B.P. Nazarenko, and V.M. Puzikov, *Fiz. Nizk. Temp.* **30**, 1302 (2004).
10. V.V. Eremenko, S.L. Gnatchenko, I.S. Kachur, V.G. Piryatinskaya, A.M. Ratner, V.V. Shapiro, M.B. Kosmyna, B.P. Nazarenko, and V.M. Puzikov, *Ukr. J. Phys.* **B49**, 432 (2004).
11. A.M. Ratner, *Phys. Rep.* **269**, 197 (1996).
12. I.Ya. Fugol', *Adv. Phys.* 27, 1 (1978).
13. G. Oversluizen, and R. Metselaar, *J. Phys. C: Solid State Phys.* **15**, 4869 (1982).
14. H.B. Dietrich, A.E. Purdy, R.B. Murray, and R.T. Williams, *Phys. Rev.* **B8**, 5894 (1973).
15. E.D. Aluker and D.J. Lusis, *Phys. Status Solidi* **A19**, 759 (1973).
16. E.D. Aluker, D.Yu. Lusis, and S.A. Chernov, *Electronic Excitations and Radioluminescence of Alkali Halide Crystals*, «Zinatne», Riga (Latvia), 1979 (in Russian).
17. A.M. Ratner, *Phys. Lett.* **A298,** 422 (2002).